

Icosahedral 13-Atom Gold Clusters: A Mathematical and Crystallographic Exercise

(recast and extended draft)

Hans Hermann Otto

Materials Science and Crystallography, Clausthal University of Technology,
Clausthal-Zellerfeld, Lower Saxony, Germany

E-mail: hhermann.otto@web.de

Abstract

Au_{13} clusters are considered as elementary building units for the formation of bigger gold nanocrystals. Two concepts for a 13-atom gold cluster have been worked out in order to compensate the mismatch between atomic radius of Au and circumsphere diameter of the icosahedron as limiting atomic distance. The first concept deals with small deviations of the outer shell gold atoms of the icosahedral nanocluster from spherical atomic shape by maintaining the size. The second one proposed a different size of shell atoms in contrast to the central atom. This concept is supported by the recently published experimental evidence for the existence of a body-centered cubic structure of gold at high pressure besides the face-centered one. The density of the gold nanocluster is found to be a little bit smaller than the density of face-centered cubic gold. The elementary icosahedral Au_{13} cluster may be considered as mediator between BCC and FCC structure. An open question is whether Au_{13} clusters are present in dense packing structures of molten gold. Applications of Au_{13} gold clusters are considered.

Keywords: Polyhedron, Platonic Solids, Mackay-Polyhedrons, Fibonacci Numbers, Golden Mean, Volume-Area Ratio, Polyhedral Void Space, Cluster Density, Cluster Formation, Au_{13} , Au_{17} .

1. Introduction

In 1962 Mackay reported about of a dense non-crystallographic packing of equal spheres and initiated the research on such icosahedral clusters [1]. The icosahedron belongs to the 5 *Platonic* solids [2] [3]. It is a convex regular polyhedron in three-dimensional *Euclidian* space and consists of 20 congruent equilateral triangular faces (F), 12 vertices (V) and 30 edges (E). These geometric elements obey the *Euler* relation $V + F - E = 2$ [4]. We are interested in the 13 atom cluster consisting of a first shell of 12 atoms of gold completed with an atom located at the center. Generally, the number of atoms building complete icosahedral clusters results in a series of special numbers C according to

$$C(n) = \frac{10n^3 - 15n^2 + 11n - 3}{3} \quad (1)$$

One obtains for the first members

$$C(1) = 1 \quad C(2) = 13 \quad C(3) = 55 \quad C(4) = 147 \quad (2)$$

where the first three numbers are *Fibonacci* numbers, but the fourth one is not. *Fibonacci* numbers are derived and introduced by *Pisano* around the year 1202 [5]. About the significance of especially number 13 for life, physics and cosmos the reader may follow a recent contribution [6].

Referring to Au_{13} and bigger gold nano-assemblies we speak more general about *AuNCs*. Their small size caused significant quantization to the conduction band leading to photonic properties and native luminescent properties allowing biomedical applications, for instance as therapy tool in cancer treatment [7]. However, in this contribution we deal with bar clusters without stabilizing ligand shells.

In the following we present a mathematical and crystallographic exercise for a better understanding of the important icosahedral clusters consisting of 13 gold atoms. Two concepts were worked out: 1. all atoms have the same size, but somewhat different shape, 2. the shell atoms are somewhat bigger than the central atom. We have calculated effective cluster diameters in comparison with the experimental value and the density of clusters as well as the void space. About greater gold clusters, for instance chiral *I-Au₆₀* gold fullerenes, see reference [8]. The Au_{13} cluster seems to be the stable early cluster that mediates as seed the coalescence and formation of Au-nanocrystals [9]. Some time ago the present author reported about the formation and application of atomically flat highly reflecting micro-platelets of Au, grown in lead bismuth germanate melt in a gold crucible [10] [11].

2. Conclusion from the Existence of a BCC Gold Structure

The recently verified existence of body-centered cubic gold under shock compression at 225 GPa comes as a great surprise [12] [13], because 8-coordinated bcc gold hardly represents a tightly packed structure, if the $Z = 2$ gold atoms are considered as equivalent entities. The density of gold at the named pressure is about 28 (gcm^{-3}). The more open bcc crystal structure with lattice parameter a is characterized by the mismatch of the atomic distance of $\frac{\sqrt{3}}{2}a = 0.8660a$ along the body diagonal and the full lattice parameter distance along the unit-cell axis. This mismatch condition means that hard spheres are not able to form a stable BCC lattice. However, in order to overcome this mismatch the size of both atoms could be varied by charge transfer tentatively generating Au^{1+} and Au_{12}^{1-} . The oxidation state of 1+ was frequently found in Au nanoparticles. The concept of gold atoms of different size could also be applied to the 13-atom icosahedral gold cluster. This leads us to believe that the central atom could have a smaller size than the shell atoms to overcome the intrinsic mismatch of icosahedral geometry as explained in the next two chapters.

The modifications of gold can be compared to the similar iron modification: α -Fe (ferrite, < 912°C, bcc-structure, $a = 2.8665 \text{ \AA}$) and γ -Fe (austenite, >912°C, fcc-structure, $a = 3.572(5) \text{ \AA}$ extrapolated to 20°C). Recently, Fe_{13} clusters with closed shell electron configuration have been reported by *Scott et al.* [14].

3. Properties of the Icosahedron

The icosahedron is a regular solid obeying non-crystallographic fivefold symmetry. The polyhedron notation is given by the symbol $[\mathbf{p}_i^{F_i}]$, where p is the polygon multiplicity and F is the number of faces. The notation is $[\mathbf{3}^{20}]$. Platonic solids can be drawn and dynamically visualized using for instance the software found under <http://drajmarsh.bitbucket.io>. However, the reader may construct the icosahedron with the help of coordinates for the vertices given in **Table 1**, where φ is the golden mean

$$\varphi = \frac{\sqrt{5}-1}{2} = 0.6180339887 \dots \quad \Phi = \frac{\sqrt{5}+1}{2} = \varphi^{-1} = \varphi + 1 = 1.6180339887 \dots \quad (3)$$

But division of all coordinates by φ would transfer ± 1 to big $\pm\Phi = \pm\varphi^{-1}$ and $\pm\varphi$ to ± 1 . These values were sometimes given in literature.

Table 1. Coordinates of Vertices for the Icosahedron and Pentagonal Dodecahedron
(Both solids are centered at the origin and suitably scaled for sake of simplicity)

Edge length: $a = 2\varphi$					
Regular icosahedron			Regular pentagonal dodecahedron		
x	y	z	x	y	z
0	$\pm\varphi$	± 1	± 1	± 1	± 1
$\pm\varphi$	± 1	0	0	$\pm\varphi^{-1}$	$\pm\varphi$
± 1	0	$\pm\varphi$	$\pm\varphi^{-1}$	$\pm\varphi$	0

Figure 1 illustrated the rotated icosahedron in order to show the fivefold axis. The central atom has a coordination of 12 in contrast to the shell atom with asymmetric $5 + 1$ coordination. This means that the atoms at the two different positions should show slightly different properties.

Important geometric relations for the icosahedron are summarized below [15]. We use the notation V_p polyhedron volume, V_{sph} in-sphere volume, A_p polyhedron surface area, A_{sph} in-sphere area, r_{circ} circumsphere radius, r_i in-sphere radius, a polygon edge length.

$$V_p = \frac{5}{6}\varphi^{-2}a^3 = 2.1816945 \cdot a^3 \quad (4)$$

$$r_{\text{circ}} = \frac{\sqrt{3+\varphi}}{2} a = 0.951056516 \cdot a \quad (5)$$

$$\approx \frac{a}{2} \cdot \left(15 - \frac{6}{\pi}\right)^{1/4} \quad (5a)$$

$$r_i = \frac{\varphi^{-2}}{2\sqrt{3}} a = \mathbf{0.755761313 \cdot a} \quad (6)$$

$$V_{sph} = \pi \cdot \frac{\varphi^{-6}}{18\sqrt{3}} a^3 \quad (7)$$

$$\frac{V_{sph}}{V_p} = \pi \cdot \frac{\varphi^{-4}}{15\sqrt{3}} = \pi \cdot 0.263814507 = 0.8287977 \approx \frac{\pi}{2 \cdot 13} \varphi^{-4} \quad (8)$$

$$A_p = 5 \cdot \sqrt{3} a^2 = 8.660254 \cdot a^2 \quad (9)$$

$$A_{sph} = \pi \frac{\varphi^{-4}}{3} a^2 \quad (10)$$

$$\frac{A_{sph}}{A_p} = \pi \cdot \frac{\varphi^{-4}}{15\sqrt{3}} \approx \frac{\pi}{2 \cdot 13} \varphi^{-4} \quad (11)$$

$$\frac{V_p}{A_p} = \frac{\varphi^{-2}}{6\sqrt{3}} = \frac{r_i}{3} \quad (12)$$

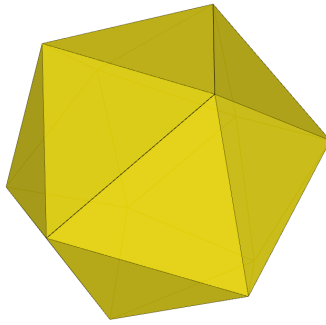


Figure 1. Illustration of an icosahedron showing one of the fivefold axes.

Also the following important golden mean angle relations may be useful for our exercise

$$\frac{\sin(36^\circ)}{\sin(72^\circ)} = \varphi \quad \sin(72^\circ) = r_{circ} \quad (13a,b)$$

$$\cos(72^\circ) = \frac{\varphi}{2} \quad \cos(36^\circ) = \frac{1}{2\varphi} \quad (13c,d)$$

$$\tan(36^\circ) = 2\varphi^2 r_{circ} \quad (13e)$$

4. The 13-Atom Gold Cluster

From the lattice parameter of face-centered cubic gold of $a_{fcc} = 4.0786 \text{ \AA}$ at 20°C we can obtain the atomic radius of gold

$$r_{Au} = \frac{4.0786}{\sqrt{2}} \text{ \AA} = 1.442 \text{ \AA} \quad r_{Au}^3 \approx 3 \text{ \AA}^3 \quad (14)$$

However, a somewhat smaller parameter as developed from the cubic lattice parameter of gold may be possible due to the decrease of atomic radii with decreasing coordination number.

If we would have an icosahedral shell of only 12 gold atoms without a central atom, the cluster diameter would yield by applying $\mathbf{a} = 2 \mathbf{r}_{Au}$

$$2(\mathbf{r}_{circ} + \mathbf{r}_{Au}) = 2 \cdot (1.902113 + 1) \cdot \mathbf{r}_{Au} = 8.30 \text{ \AA} \quad (15)$$

If the center is occupied to assemble a 13-atom cluster by maintaining the atomic volume of gold, the outer atomic shell suffer an atomic deformation from spherical to slightly pancake form to compensate for the mismatch caused by the fact that \mathbf{r}_{circ} is a little bit smaller than \mathbf{a} (equation 5). The mismatch caused a strain towards the polyhedron center. You can also follow the mismatch considering the in-sphere radius of the icosahedron \mathbf{r}_i , which is smaller than the high \mathbf{h}_T of a tetrahedron as an example for a dense sphere packing

$$\mathbf{r}_i = 0.755761313 \cdot \mathbf{a} \quad (16)$$

$$\mathbf{h}_T = \frac{\sqrt{6}}{3} \cdot \mathbf{a} = 0.816496 \cdot \mathbf{a} \quad (17)$$

We proceed with the derivation of the small outer shell atomic deformation of a 13-atom icosahedral Au cluster. The formula for an elliptical deformed sphere with equal volume as the sphere is

$$V = \frac{4\pi}{3} \mathbf{c}_1^2 \mathbf{a}^2 \cdot \mathbf{c}_2 \mathbf{a} \quad \text{with} \quad \mathbf{c}_2 = \frac{1}{\mathbf{c}_1^2} \quad (18)$$

On can obtain a matching numerical result between the free halve-diagonal distance \mathbf{r}_{eff} and the needed atomic space for an outer atom and the central atom

$$\mathbf{r}_{eff} = \mathbf{c}_1 \cdot 2\mathbf{r}_{Au} \cdot \mathbf{r}_{circ} \quad (19)$$

$$\mathbf{r}_{eff} = \mathbf{c}_2 \cdot \mathbf{r}_{Au} + \mathbf{r}_{Au} = \left(1 + \frac{1}{\mathbf{c}_1^2}\right) \mathbf{r}_{Au} \quad (20)$$

Both equations result in a cubic equation with respect to the parameter \mathbf{c}_1

$$\mathbf{c}_1^3 - \frac{\mathbf{c}_1^2}{2\mathbf{r}_{circ}} - \frac{1}{2\mathbf{r}_{circ}} = 0 \quad (21)$$

The solution provided for the ellipsoid axes parameters

$$\mathbf{c}_1 = 1.0255718 \quad (22)$$

and

$$\mathbf{c}_2 = 0.95075333 \quad (23)$$

From a number theoretical view c_1 can vice versa be approximated by

$$c_1 \approx \sqrt[3]{\frac{13}{12}} = 1.02704 \quad (24)$$

Finally, we obtain matching distances

$$c_1 \cdot 2r_{Au} \cdot r_{circ} = 2.809085 \text{ \AA} \quad (25)$$

$$c_2 \cdot r_{Au} + r_{Au} = \left(1 + \frac{1}{c_1}\right) r_{Au} = 2.809085 \text{ \AA} \quad (26)$$

Then the cluster diameter d_{13} can be calculated to be

$$d_{13} = 4r_{Au}c_1r_{circ} + 2r_{Au}c_2 = 8.356 \text{ \AA} \quad (27)$$

This result agrees well with the cluster diameter observed experimentally: $d_{13}(exp) = 84 \text{ pm} = 8.4 \text{ \AA}$ [16].

5. Density Considerations

We ask what the density of the cluster is in comparison with crystalline gold. Gold crystallizes in the face-centered cubic crystal structure with lattice parameter $a_{fcc} = 4.0786 \text{ \AA}$ and $Z = 4$ atoms in the unit cell, it has a calculated density D_x of

$$D_x = \frac{Z \cdot M}{V_u \cdot N_A} = \frac{4 \cdot 196.9665}{4.0786^3 \cdot 10^{24} \cdot 0.602214 \cdot 10^{-24}} = 19.2827 \text{ gcm}^{-3} \quad (28)$$

where M is the molar weight and N_A is *Avogadro's* number.

For the 13-atom gold cluster we obtain in a similar way by adequate weighting of the 12 shell atoms an effective Z of about 3 atoms. For sake of simplicity we replace the volume contribution of the shell atoms by spherical cut-outs instead of five-sided pyramids capped with spherical sections. Therefore the base area A of the pyramid is replaced by a circle having an effective radius r_{eff}

$$A = \frac{5}{4} \tan(54^\circ) \cdot r_{Au}^2 = \pi r_{eff}^2 \quad (29)$$

$$r_{eff} = 0.74003038 \cdot r_{Au} \quad (30)$$

The height of the sphere section is

$$h = r_{Au} \left(1 - \sqrt{1 - \frac{5}{4\pi} \tan(54^\circ)}\right) = 0.327427 \cdot r_{Au} \quad (31)$$

The formula for the cut-out volume yields

$$V_{cut} = \frac{2\pi}{3} r_{Au}^2 \cdot h = 0.68576 \cdot r_{Au}^3 \quad (32)$$

$$\frac{V_{cut}}{V_{Au}} = \frac{2\pi}{3} \cdot \frac{3}{4\pi} \cdot 0.327427 = 0.163713 \approx \frac{1}{6} \quad (33)$$

With this result we obtain only about 3 gold atoms hosting in the icosahedron

$$12 \cdot \frac{V_{cut}}{V_{Au}} + 1 = 2.965 \approx 3 \quad (34)$$

It gives too small a density of the gold cluster of

$$D_{cluster} \approx 17.25 \text{ (gcm}^{-3}\text{)} \quad (35)$$

However, when using the original icosahedron volume by eliminating the factor c_1^3 , we get for the density

$$D_{cluster} = \frac{3 \cdot 196.9665}{52.3335 \cdot 10^{24} \cdot 0.602214 \cdot 10^{-24}} = 18.75 \text{ (gcm}^{-3}\text{)} \quad (36)$$

This density approach, based on the cluster diameter of still 8.30 Å (relation 15), supposes that the size of the central gold atom within the cluster is reduced a little bit by suffering an internal pressure (chemical pressure) in contrast to the shell atoms.

Now we use the second approach where the shape of the shell atoms is varied, but the volume of all atoms remains unchanged. If we define the volume that completely contains all 13 gold atoms, we must choose the icosahedron edges as tangents to the shell atoms. This means that the half-diameter of the cluster have to be enhanced by a length of Δl , approximately obtained as

$$\Delta l \approx \left(\frac{1}{\sin^2 \gamma} - 1 \right) \cdot c_2 \cdot r_{Au} = 0.2928 \text{ Å} \quad (37)$$

where $\gamma = 110.90515^\circ$ is the angle between edge and face of the icosahedron.

Then we obtain for the edge length of this enhanced icosahedron

$$a' = \frac{d_{13} + 2\Delta l}{\sqrt{3 + \varphi}} = 4.70 \text{ Å} \quad (38)$$

and for the volume respectively

$$V = \frac{5}{6\varphi^2} a'^3 = 226.51 \text{ Å}^3 \quad (39)$$

But we should reduce this volume by the volume of the produced pyramidal peaks about the 12 shell atoms. The small peak volume for the 12 shell atoms is about

$$12 \cdot V_{peak} = 5 \cdot \tan(54^\circ) \cdot \tan^2(55.45^\circ) \cdot \varphi^2 \cdot (\Delta l)^3 \approx 0.162 \text{ Å}^3 \quad (40)$$

Then the density of the cluster provides the following lower estimate

$$D_{cluster} = \frac{Z \cdot M}{V \cdot N_A} \geq \frac{13 \cdot 196.9665}{226.35 \cdot 10^{24} \cdot 0.602214 \cdot 10^{-24}} = 18.78 \text{ (gcm}^{-3}\text{)} \quad (41)$$

The volume ratio of the gold atoms to the icosahedron volume yields

$$\frac{V_{Au}}{V_P} \approx \frac{3 \cdot \frac{4\pi}{3} r_{Au}^3}{8 \cdot \frac{5}{6} \varphi^{-2} r_{Au}^3} = \frac{3\pi\varphi^2}{5} = 0.7200 \quad (42)$$

and the void volume ratio respectively

$$1 - \frac{V_{Au}}{V_P} = 0.23542 \approx \varphi^3 = 0.2800 \quad (43)$$

Comparable values for the face-centered cubic gold are

$$\frac{V_{Au}}{V_{fcc}} = \frac{4 \cdot \frac{4\pi}{3} r_{Au}^3}{16 \cdot \sqrt{2} \cdot r_{Au}^3} = \frac{\pi}{\sqrt{2} \cdot 3} = 0.74048 \quad (44)$$

$$1 - \frac{V_{Au}}{V_{fcc}} = 0.259519 \approx 1 - \sqrt[3]{2} = 0.25952 \quad (45)$$

It indicates again that the packing efficiency of the icosahedral cluster is only marginally smaller than that for the face-centered cubic lattice.

The density of solid gold just below the melting point at $T_m = 1064^\circ\text{C}$ is about 18.31 (gcm^{-3}) and that of liquid gold above the melting point is about 17.31 (gcm^{-3}) [17]. One may argue to find 13-atom gold clusters as dense building entities in molten gold. The transformation of gold exhibiting the body-centered cubic structure into the face-centered cubic one may be via a liquid state composed in part of elementary Au_{13} units. The 13-atom cluster with a 12-coordinated central atom can be regarded as mediator between the eightfold coordinated BCC structure and the twelfold coordinated FCC structure. A hard-sphere respectively soft sphere transformation simulation was recently reported [18]. The reader may also study an early contribution to structural components of molten gold published by *Richter and Breitling* [19].

A fictive hard-sphere lattice parameter of BCC gold can be calculated using the atomic radius of gold. We obtain for the lattice parameter at ambient conditions

$$a_{bcc} = \frac{4}{\sqrt{3}} r_{Au} = 3.330 \text{ \AA} \quad (46)$$

and for the fictive density

$$D_{bcc} = \frac{2 \cdot 196.9655}{36.931 \cdot 0.602214} = 17.712 \text{ (gcm}^{-3}\text{)} \quad (47)$$

If we tentatively apply the thermal expansion coefficient for FCC gold, reported as $\alpha_{Au} = 13.4 \cdot 10^{-6} (\text{°C}^{-1})$ [20], we calculated for the fictive density just below the melting point a value of

$$D_{bcc}^{fic}(T_m) \approx 17.00 (\text{gcm}^{-3}) < D_{melt} \approx 17.31 (\text{gcm}^{-3}) \quad (48)$$

This explains the non-existence of BCC gold under ambient conditions in contrast to the relative stable Au_{13} nanocluster, whereas under high-pressure conditions due to a fortunate pressure coefficient BCC gold and its transformation into FCC gold respectively the Au_{13} cluster could be observed [18].

6. IrAu₁₂ Cluster

Recently, it was reported about the synthesis and properties of nearly perfect icosahedral IrAu₁₂ clusters showing superior photoluminescence [21]. Because the central Ir atom has a smaller atomic radius of 1.357 Å compared to Au, the mismatch is considerably reduced. In the reference the following atomic distances were experimentally determined [21]

$$Ir - Au = 2.740 \text{ \AA} \quad Au - Au = 2.881 \pm 0.028 \text{ \AA} \quad (49)$$

$$\frac{1.357+1.442}{2 \cdot 1.442} = 0.9712 > 0.9510 = \frac{\sqrt{3+\phi}}{2} \quad (50)$$

The best choice would be vanadium as central atom of the gold icosahedron with an atomic radius of about 1.311 Å leading to a mismatch of only $0.95458-0.95106 = 0.0035$, or copper with 1.278 Å giving $0.94379-0.95106 = -0.0073$.

7. Characteristics of X-Ray Scattering from Hollow Polyhedral Structures

Some years ago, the present author modeled a cubic cuprate super-cage and calculated its X-ray powder pattern [22]. The pattern showed a pronounced intensity modulation of the peaks, which can be understood as resulting from a uniform electron density distribution ρ on the shell of a hollow sphere of radius r_s , approximating the empty polyhedral cage. This concept can be applied also to icosahedral Au_{13} clusters.

By calculating the structure factor $F(\mathbf{k})$ as the Fourier transform of the radial charge density $\rho(r)$, the property of the Dirac delta function δ is used, where the integral of δ times some other function $f(r)$ is equal to the value of $f(r)$ at the position of δ :

$$\int f(r)\delta(r-R)dr = f(R). \quad (51)$$

Following in part the calculation concept of *Alloul & Lyle* [23] applied to C_{60} buckyballs, one obtains the scale factor A from the total number N_e of electrons of the polyhedron, confined to a shell of radius R as

$$N_e = \int \rho(r) d^3r = \int_0^\infty 4\pi r^2 \delta(r-R) A dr = 4\pi AR^2, A = N_e / (4\pi R^2). \quad (52)$$

Using polar coordinates r, φ, θ , for spherically symmetric functions, one obtains for the volume element

$$d^3r = r^2 dr d\varphi \sin(\theta) d\theta. \quad (53)$$

Then the *Fourier* transform yields

$$F(\mathbf{k}) = \int \rho(r) \exp(-i\mathbf{k}\cdot\mathbf{r}) d^3r \quad (54)$$

$$= A \int_0^\infty r^2 \delta(r-R) dr \int_0^{2\pi} d\varphi \int_0^\pi \exp(-ikr \cos \theta) \sin \theta d\theta \quad (55)$$

Substituting $\cos(\theta) = \zeta$ gives

$$\int_0^\pi \exp(-ikr \cos \theta) \sin \theta d\theta = \int_{+1}^{-1} (-1) \exp(-ikr\zeta) d\zeta = 2 \frac{\sin(kr)}{kr} \quad (56)$$

Hence

$$F(\mathbf{k}) = 4\pi A \int_0^\infty \frac{\sin(kr)}{kr} r^2 \delta(r-R) dr = 4\pi AR^2 \frac{\sin(kR)}{kR} = N_e \frac{\sin(kR)}{kR} \quad (57)$$

Finally, the intensity results as

$$I(\mathbf{k}) = |F(\mathbf{k})|^2 = N_e^2 \left(\frac{\sin(kR)}{kR} \right)^2 \quad (58)$$

By replacing $|\mathbf{k}| = k = 2\pi/d$ with the interplanar spacing $d = \lambda/(2\sin(\theta)) = a/(\sqrt{h^2+k^2+l^2})$ exemplarily for a body-centered cubic crystal, it can be seen that $I(\mathbf{k})$ shows zeros for $R/d = n/2$ with integer n and maxima near $R/d = (2n+1)/4$, respectively. A more exact solution, reflecting the slope of the denominator function, may be applied to calculate the radius R from d or k values assigned to the ‘corrected’ maxima of order n :

$$R = k^{-1} f(z) = k^{-1} (z - z^{-1}), \quad (59)$$

where

$$z = \pi \left(\frac{2n+1}{2} \right). \quad (60)$$

In addition, the intensity $I(\mathbf{k})$ of an actual ‘powder’ pattern has to be corrected for LpG factors and overall atomic displacement $\exp(-2T)$, respectively. This was applied in [Figure 2](#) to display the modulated intensity of the bar icosahedral Au_{12} cage structure. Adding the central gold atom would cause only a slight perturbation of the obtained result.

The first maximum on [Figure 2](#) is seen at $k = 1.601 \text{ \AA}^{-1}$. We can reproduce the radius R of the cluster for $n = 1$ by using the relations (59) and (60) being $R = 2.81 \text{ \AA}$. For sake of comparison, the location of the 111 and 200 reflections of face-centered cubic gold are displayed in [Figure 2](#) in blue color at $|k| = 2.668 \text{ \AA}^{-1}$ respectively $|k| = 3.028 \text{ \AA}^{-1}$, settled

both in the second spherical shell diffraction ripple. The first diffraction fringe is not occupied attributed to the selection rules for face-centered cubic lattices.

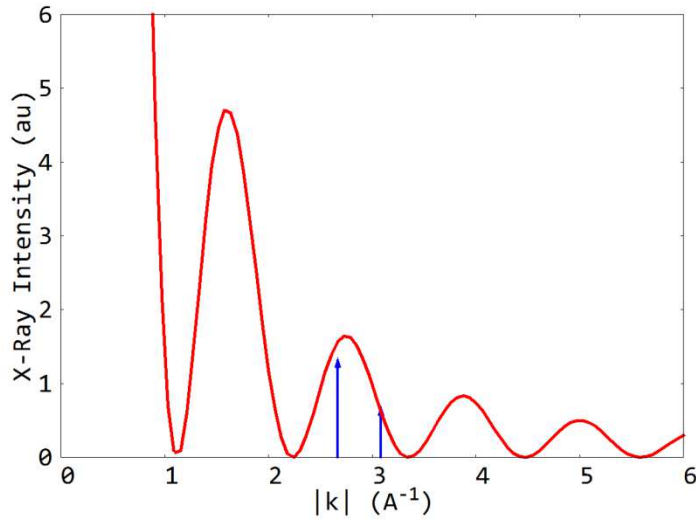


Figure 2. Simulation of the X-Ray Intensity Distribution of an Spherical Shell Icosahedral Au₁₂ Cage Structure (arbitrary intensity units, scattering vector $|k| = \frac{2\pi}{d}$, $R = 2.81 \text{ \AA}$). The blue lines display the location of the 111 and 200 reflections of fcc gold.

6. Nanocluster Formation Forces

Among the forces involved in the formation of nanoclusters, the driving out of the all-pervading vacuum energy field (*Casimir* force) must be named first [24]. Once elementary icosahedral Au₁₃ clusters are formed under ambient conditions, they can serve as seeds around which different bigger gold nanocrystals evolve [9].

The ligand stabilized Au₁₃ cluster always shows the closed electron shell superatomic orbital configuration (1S)²(1P)⁶. On the other side, by considering the next closed shell we have a connection with number 13

$$8 + 18 = 2 \cdot 13 \quad (61)$$

7. Extended Applications

The photonic properties of icosahedral gold clusters with native luminescence have been successfully used in biomedical applications as therapy tool in cancer treatment [7]. Besides such applications, ligand stabilized icosahedral 13-atom gold clusters assembled in capillaries are conceivable to generate amplified spontaneous emission and lasing and would promise a quite stable facility. A recent example for such application is the generation of random lasing in capillaries doped with rhodamine 6G-microspheres [25]. Exceptional optical and electronic properties are suggested by the possibility that Au¹⁺ host in the center of the 13-Au icosahedral cluster.

Recently, the synthesis of atomically precise Au₁₃ nanoclusters were performed via catalytic reduction of Au⁺¹ to Au⁰ by activated H₂ using a palladium catalyst [26]. Also the potential of such clusters for CO₂ reduction is there reported.

Very interesting from the viewpoint of crystallography as well as applications is the observed helical charge movement in [Au₁₃P₁₀Cl₂]³⁺ clusters caused by a slight torsion between both equatorial Au₅ pyramids of the icosahedron [27]. Could such a twist also be generated, when the icosahedron suffers a moderate pressure along a fivefold axis?

Another question is in what form nanoscale gold is primary deposited, when gold eating bacteria like cupriavidus metallidurans keep health by pumping out an excess of that toxic metal? Could along this route Au₁₃ gold clusters be produced in large-scale amount?

8. Magic Au₁₇ Nanocluster

The icosahedron with point group symmetry I_h can be build up from two pentagonal pyramids where one pyramid is 180° rotated around a vertical axis and then both pyramids are connected by equilateral triangles. However, when four pentagonal pyramids connect their sides by squares, and the cage center is occupied by an additional atom, then a beautiful and magic Au₁₇ cluster with non-crystallographic D_{4d} point group symmetry is formed, showing an improper S_8 axis. Another example for this point group symmetry is the puckered ring of octasulfur. Number 17 can be obtained as the mean of the successive *Fibonacci* numbers 13 and 21. Such assembly of Au atoms allows in contrast to the icosahedral one more space for the central atom. The distance between central and peak atom match now almost perfectly the space needed for an Au atom

$$r_{circ} = r_{Au} + 2 \cdot r_{Au} \sqrt{1 - \frac{1}{(3+\varphi)\varphi^2}} = 2.0515 \cdot r_{Au} \quad (62)$$

The cluster diameter yields

$$d_{17} = 2r_{circ} + 2r_{Au} \approx 8.80 \text{ \AA} \quad (63)$$

The dominance of such superatomic clusters with geometric and electronic shell closure was experimentally and theoretically verified for Ag₁₇ clusters by Yin et al. [28]. The results can be applied to Au₁₇ clusters, too. Recently, unexpected other Au₁₇ clusters were investigated with star-like forms [29].

9. Electron and 13-Atom Cluster

We proposed the vortex structure of the electron being an icosahedral *Moebius* ball, where closed spiraling waves travel inwardly and outwardly along *Moebius* slings thereby touching the 12 vertices and the center [30] [31]. These positions are equivalent to the atomic position of the 13-atom gold cluster. This magic body unifies beauty and effectiveness. We connected icosahedron mathematics with number 13 and the fifth power of the golden mean as well as *Sommerfeld's* universal structure constant $\alpha^{-1} = 137.036$ for rotational movement and the

gyromagnetic factor of the electron g_e . Some equations should demonstrate such numerical interrelations [32] [33]

$$d_{circ}^4 = 13 + \varphi^5 \quad (64)$$

$$\frac{4}{5} \left(13 + \frac{1}{13}\right)^2 + \varphi^3 = 137.0407 \quad (65)$$

$$137 + \frac{2}{5} \varphi^5 = 137.03606 \quad (66)$$

$$\alpha^{-1} = 4\pi^3 + (\pi + 1)\pi = 137.0363 \quad (67)$$

$$\sqrt{2\varphi/\alpha} = 13.01482999 \dots \approx (\pi + 1)\pi = 13.011197 \quad (68)$$

$$g_e = 2 + \frac{\varphi^6}{24} - \frac{1}{2} \left(\frac{\varphi^6}{24}\right)^2 - \frac{1}{4} \left(\frac{\varphi^6}{24}\right)^3 = 2.002319304 \dots \quad (69)$$

However, the exact derivation of g_e matching the exorbitantly accurate experimental value was given by *Gwynn* [34].

We should recognize some similarities between the structures of electron, atom and superatom.

10. Conclusion

The icosahedral cluster consisting of 13 atoms of gold represents a dense solid body that is only 2.6 % less dense than face-centered cubic gold with its dense sphere atomic packing. The 12 shell atoms of the 13-atom cluster can deviate slightly from assumed spherical shape, in this way compensating the geometrical mismatch that is caused by the occupation of the center by an additional atom. The shell atoms can be approximated by an elliptically shaped influence sphere having two equal half-axes enlarged by the factor of 1.02557, and the third axis reduced by the factor of 0.95075. Another possibility is to attribute slightly different sizes for the central atom and the shell atoms. This approach may be supported by the existence of body-centered-cubic gold at high pressure. Under ambient conditions the Au_{13} cluster serves as seed, around which bigger nanocrystals of gold evolve. It should be investigated further, whether icosahedral Au_{13} clusters are formed in molten gold as dense packing alternative. Since *Mackay's* approach of non-crystallographic packing of spheres many important biomedical applications of such clusters with ever new possibilities have exceeded all expectations. We would like to conclude with the slogan '*make gold golden*'.

Conflicts of Interest

The author declares no conflict of interests regarding the publication of this paper.

References

- [1] Mackay, A. L. (1962) A dense noncrystallographic packing of equal spheres. *Acta Crystallographica* **15**, 916-918
- [2] Archer-Hind, R. D. (1888) The Timaeus of Plato. *MacMillan and Co*, New York.
- [3] Field, J. V. (1997) Rediscovering the Archimedean Polyhedra: Piero della Francesca, Luca Pacioli, Leonardo da Vinci, Albrecht Dürer, Daniele Barbaro, and Johannes Kepler. *Archive for History of Exact Sciences* **50**, 241-289.
- [4] Euler, L. (1752) Elementa doctrine solidorum. *Novi commentarii academiae scientiarum imperialis petropolitanae* **4**, 109-160.
- [5] Pisano, L. (1202) Fibonacci's Liber Abaci (Book of Calculation). Biblioteca a Nazionale di Firenze.
- [6] Otto, H. H. (2025) What Tells Geometrical Reciprocity about Mass Constituents of the Universe and the Universe itself? *Researchgate.net*, 1-35
- [7] Van de Looij, S. M., Hebels, E. R., Viola, M., Hembury, M., Oliveire, S., and Vermonden, T. (2021) Gold Nanoclusters: Imaging, Therapy, and Theranostic Roles in Biomedical Applications. *Bioconjugate Chemistry* **33**.
- [8] Mullins, S.-M. et al. (2017) Chiral symmetry breaking yields the I-Au₆₀ perfect golden shell of singular rigidity. *Nature Communications* **9**, 3352.
- [9] Jin, B., Wang, V., Jin, C., De Yorea, J. J., and Tang, R. (2021) Revealing Au₁₃ as Elementary Clusters During the Formation of Au Nanocrystals. *The Journal of Physical Chemistry Letters* **12**,
- [10] Otto, H. H. and Müller-Lierheim, W. (1978) Crystal data for Pb₃Bi₂[(GeO₄)₃] *Journal of Applied Crystallography* **11**, 158-159.
- [11] Otto, H. H. (2016) Au micro-platelets: formation and application. *Researchgate*. Technical Note, 1-2.
- [12] Briggs, R. et al. (2019) Measurement of Body-Centered Cubic Gold and Melting under Shock Compression, *Physical Review Letters* **123**, 045701.
- [13] Sharma, S. M. et al. (2019) Structural Transformation and Melting in Gold Shock Compressed to 355 GPa. *Physical Review Letters* **123**, 045702.
- [14] Scott, A. G., Galico, D. A., Bogacz, I., Oyala, P. h., Yano, J., Suturina, E. A., Murugesu, M., and Agapie, T. (2023) High-Spin and Reactive Fe₁₃ Cluster with Exposed Metal Sites. *Angewandte Chemie, Int. Ed.* **62**, 202313880
- [15] Otto, H. H. (2021) Ratio of In-Sphere Volume to Polyhedron Volume of the Great Pyramid Compared to Selected Convex Polyhedral Solids. *Journal of Applied Mathematics and Physics* **9**, 41-56.
- [16] Ren, Shi-Wei (2023) The deformation of the icosahedral gold 13-atom cluster. *Modern Physics Letters B* **8**
- [17] <https://periodictable.com>
- [18] Wang, F. and Han, Y. (2019) Transformation of body-centered cubic crystals composed of hard or soft spheres to liquid or face-centered cubic crystals. *The Journal of Chemical Physics* **150**, 014504.
- [19] Richter, H. and Breiting, G. (1970) Strukturkomponenten von geschmolzenem Gold, Silber und Blei. *International Journal of Materials Research* **61**, 628-636.
- [20] Straumanis, M. E. (1971) Neubestimmung der Gitterparameter, Dichten und thermischen Ausdehnungskoeffizienten von Silber und Gold, und Vollkommenheit der Struktur. *Monatshefte für Chemie* **102**, 1377-1386.
- [21] Mutoh, K., Yakagi, T., Takano, S., Kawakita, S., Iwasa, T., Taketsugu, T., Tsukada, T. and Nakashima, T. (2025) A nearly perfect icosahedral IrAu₁₂ superatom with superior photoluminescence obtained by ligand engineering. *Chemical Science* 2025, 1-7.

- [22] Otto, H. H. (2015) Modeling of a Cubic Antiferromagnetic Cuprate Super-Cage. *World Journal of Condensed Matter Physics* **5**, 160-178.
- [23] Alloull, H. and Lyle, S. (2010) Introduction to the Physics of Electrons in Solids. E-Book, Springer Verlag.
- [24] Casimir, H. B. G. (1948) On the attraction between two perfectly conducting plates. *Proceedings of the Koninklijke nederlandse Akademie van Wetenschappen* **B51**, 793-795.
- [25] He, H., Russell-Hill, P., Blau, W. J., Kislyakov, I. M., Rosanov, N. N., Dong, N., and Wang, J. (2025) Amplified spontaneous emission and random laser generation in capillaries doped with rhodamine 6G-microspheres. *Applied Optics* **64**, 3383-3390.
- [26] Wang, Y. et al. (2025) Heterogeneous Catalytic Syntheses of Au₁₃Nanoclusters. *Chinese Chemical Society* <http://ccschem> 025.202405142
- [27] Shichibu, Y., Ogawa, Y., Sugiuchi, M. and Konishi, K. (2021) Chiroptical activity of Au₁₃clusters: experimental and theoretical understanding of the origin of helical charge movements. *Nanoscale Advances* **3**,1005-1011.
- [28] Yin, B., Du, Q., Geng, L., Zhang, H., Luo, Z., Zhou, S. and Zhao, J. (2021) Superatomic Signature and Reactivity of Silver Clusters with Oxygen: Doubly Magic Ag₁₇ - with Geometric and Electronic Shell Closure. *CCS Chemistry* **3**, 219-229.
- [29] Nhat, P. V., Si, N. T., Kiselev, V. G., Fielcke, A., Pham, H. T., and Nguyen, M. T. (2022) Unexpected structures of the Au₁₇ gold cluster: the stars are shining. *Chemical Communications* **58**, 5785-5788.
- [30] Otto, H. H. (2022) Golden Quartic Polynomial and Moebius-Ball Electron. *Journal of Applied Mathematics and Physics*, Volume **10**, 1785-1812.
- [31] Otto, H. H. (2022) Modern Arts Meets Modern Physics. *ResearchGate.net*.
- [32] Otto, H. H. (2020) Phase Transitions Governed by the Fifth Power of the Golden Mean and Beyond. *World Journal of Condensed Matter Physics* **10**, 135-159.
- [33] Otto, H. H. (2025) What Tells Geometrical Reciprocity about Mass Constituents of the Universe and the Universe itself? *ResearchGate.net*, 1-34.
- [34] Guynn. P. (2018) Thomas precession is the basis for the structure of matter and space. *viXra*: 1810.0456, 1-27.